

1 **Full title:** Using proper mean generation intervals in modelling of COVID-19

2

3 Xiujuan Tang<sup>1</sup>, Salihu S. Musa<sup>2,3</sup>, Shi Zhao<sup>4,5</sup>, and Daihai He<sup>2,\*</sup>

4 <sup>1</sup> Shenzhen Center for Disease Control and Prevention, Shenzhen, Guangdong, China

5 <sup>2</sup> Department of Applied Mathematics, The Hong Kong Polytechnic University, Hong Kong, China

6 <sup>3</sup> Department of Mathematics, Kano University of Science and Technology, Wudil, Nigeria

7 <sup>4</sup> JC School of Public Health and Primary Care, Chinese University of Hong Kong, Hong Kong, China

8 <sup>5</sup> Shenzhen Research Institute of Chinese University of Hong Kong, Shenzhen, China

9

10 \* Correspondence to: [daihai.he@polyu.edu.hk](mailto:daihai.he@polyu.edu.hk) (DH)

11

12 **Abstract**

13 In susceptible-exposed-infectious-recovered (SEIR) epidemic models, with the exponentially  
14 distributed duration of exposed/infectious statuses, the mean generation interval (GI, time lag between  
15 infections of a primary case and its secondary case) equals the mean latent period (LP) plus the mean  
16 infectious period (IP). It was widely reported that the GI for COVID-19 is as short as 5 days. However,  
17 many works in top journals used longer LP or IP with the sum (i.e., GI), e.g., > 7 days. This discrepancy  
18 will lead to overestimated basic reproductive number, and exaggerated expectation of infectious attack  
19 rate and control efficacy, since all these quantities are functions of basic reproductive number. We argue  
20 that it is important to use suitable epidemiological parameter values.

21

22 **Keywords:** COVID-19, mean generation interval, mean latent period, mean infectious period.

23

24

## 25 Introduction

26 Emerging and re-emerging infectious diseases pathogens remain an enormous issue for public  
27 health and socio-economic growth because they can spread rapidly worldwide. Coronavirus disease  
28 2019 (COVID-19), a respiratory disease, caused by the severe acute respiratory syndrome coronavirus 2  
29 (SARS-CoV-2) (Li et al., 2020; WHO, 2021), has been a tremendous public health problem affecting  
30 every corner of the world (WHO, 2021). Since its appearance in late 2019, about 124 million people  
31 contracted and over 2.7 million died worldly as of 25 March 2021 (WHO, 2021). Until recently, many  
32 clinical features and underlying etiology of the SARS-CoV-2 remain unclear. Timely treatment and  
33 effective non-pharmaceutical interventions (NPIs) control measures against disease is important for  
34 timely mitigation (WHO, 2021).

35 Generation interval (GI), which can also be referred to as the generation time, is the time lag  
36 between infection incidents in an infector-infectee pair (Svensson, 2007). It is a proxy of serial interval  
37 (SI) of infectious disease, which is the time lag between onsets of the symptoms in an infector-infectee  
38 pair (Ali et al., 2020). The SI and GI are vital biological quantities (epidemic parameters) used for  
39 estimating the basic reproductive number (denoted by  $R_0$ ) which is defined as the number of secondary  
40 cases that one infected person will generate on average over the course of his/her infectious period in a  
41 population that is completely susceptible (Li et al., 2020; Musa et al., 2020a), as well as time-varying  
42 basic reproduction number,  $R_0(t)$ , which determines the average number of secondary cases per  
43 infectious case in a population made up of both susceptible and non-susceptible hosts (Ali et al., 2020).  
44 Moreover, the importance of GI is also reflected in the renewal equation  $R_0(t) = \frac{I_t}{\sum I_{t-k}w_k}$ , where  $w_k$   
45 represents the GI distribution,  $I_t$  denotes daily infections and  $R_0(t)$  represents the daily instantaneous  
46 reproductive number, which reflects transmission dynamics at a time,  $t$  (Park et al., 2020). Recently,  
47 many works have been done to understand and/or estimate the GI, and its proxy, i.e., SI, associated with  
48 infectious diseases, including the SARS-CoV and the SARS-CoV-2 (Ali et al., 2020; He et al., 2020b;  
49 Lipsitch et al., 2003; Nishiura et al., 2020; Svensson, 2007; Wallinga and Lipsitch, 2007; Wang et al.,  
50 2020; Zhang et al., 2020; Zhao et al., 2020b).

51 Previous reports highlighted that when the SI is larger, the uncertainty and overestimation will be  
52 higher (Ali et al., 2020; Zhao et al., 2020a). The SI (which depends hugely on the incubation period of  
53 infectious disease) can be negative if the start of the symptoms in the infectee happens earlier than the  
54 start of the symptoms in the infector (person who transmit the disease) (Du et al., 2020; Ganyani et al.,

55 2020a; Kong et al., 2020; Ren et al., 2020; Tindale et al., 2020; Zhao, 2020). The SI can also be negative  
56 when the incubation period has a wider range than the latent period, which may result in pre-  
57 asymptomatic transmission as reported in recent COVID-19 studies (Ali et al., 2020; He et al., 2020b).  
58 However, unlike SI, the GI is solely non-negative according to its definition (Wallinga and Lipsitch,  
59 2007; Yan, 2008).

60 The incubation period is the time between infection and the onset of symptoms (Yan, 2008).  
61 Although the time of exposure for an individual who transmits the disease (infector) is usually  
62 indistinguishable, the time of exposure of an individual who gets the infection (infectee) can be  
63 determined by the contact tracing history of the ‘infector-infectee’ pair. This subsequently indicates that  
64 for ‘infector-infectee’ pairs, there is a single infector that relates to the infectee epidemiologically.  
65 Hence, the incubation periods of infectees may be identifiable. However, the latent period differs from  
66 the incubation period, it is defined as the time lag between the infection in exposure and onset  
67 (beginning) of infectiousness of a typical case (Yan, 2008). Since the beginning of infectiousness is  
68 indistinguishable, the latent period is unidentifiable. Thus, we noticed that in many diseases (mostly  
69 infectious), the mean latent period is less than or equal to the mean incubation period (such as COVID-  
70 19) (Ali et al., 2020), whereas some diseases have a long latent period, e.g., Ebola virus disease. Note  
71 that people infected with Ebola are not infectious until the symptoms started, the incubation period of  
72 Ebola varies between 2-21 days).

73 Moreover, the latent period is the time interval when an infected individual is unable to transmit  
74 the disease. While the time interval during which an infected individual can transmit the disease is called  
75 the infectious period. Both are random variables and are considered independent, thus, the LP and IP are  
76 not generally traceable. However, SI is identifiable and well-studied, and reported by epidemic models  
77 (Lipsitch et al., 2003; Nishiura et al., 2020). We observed that some studies in the literature did not use  
78 the LP and IP appropriately, as the sum of their mean equals to the mean generation interval in SEIR-  
79 based models, that is, mean GI = mean LP + mean IP. Using the same notation as in (Svensson, 2007),  
80 we have that, the expectation of the random generation interval is given by  $E(T) = E(X) + E(Y)$ , where  
81  $T$  is the random variable representing the generation interval of the infection, and  $X$  and  $Y$  represent the  
82 random latent time and random infectious time, respectively. Details on this relation in the SEIR-based  
83 model can be found in Svensson (Svensson, 2007).

84 Furthermore, it is of vital importance to forecast the size of the outbreak, including infection attack  
85 rate (AR), the need for ventilators and hospital beds, the expected severe cases and deaths, the herd

86 immunity threshold, and the vaccine supply needed. All of these are associated with the time-varying  
87 basic reproductive number,  $R_0(t)$ . Given the important role of  $R_0(t)$ , it is imperative to obtain their  
88 estimation more accurately. Therefore, it is crucial to use the proper value for the mean LP and mean IP  
89 in SEIR compartmental models. In this work, we showed that longer IP or LP leads to an overestimation  
90 of reproductive number, using COVID-19 confirmed death cases data for Belgium, Israel, and the  
91 United Arab Emirates (UAE). We noticed that Belgium was hit badly by two waves. Israel and UAE  
92 have started large-scale vaccination programs. We choose these countries (as an example) to  
93 demonstrate the impact of the GI on  $R_0(t)$  to provide more qualitative insights on the use of the GI for  
94 controlling the disease outbreaks.

## 95 **Methods**

96 We use the COVID-19 reported deaths data retrieved from the official website of the World  
97 Health Organization (WHO) public surveillance reports for Belgium, Israel, and UAE available from  
98 <https://covid19.who.int/> (WHO, 2021). The time-series distribution of weekly confirmations of COVID-  
99 19 cases and deaths in Belgium, Israel, and UAE were depicted in **Figure 1** which shows the patterns of  
100 the COVID-19 epidemics in these three countries. The cases and deaths for COVID-19 are represented  
101 by black and red dotted curves respectively. We observed that Israel and UAE show similar epidemic  
102 curve patterns. While Belgium was hit harder with the two waves of COVID-19 outbreaks. The  
103 population data for the three countries were obtained from the Worldmeter, available from  
104 <https://www.worldometers.info/population/> (WM, 2021).  
105 Thus, we formulate the following simple epidemic model.

$$106 \quad \dot{S} = -\frac{\beta SI}{N},$$

$$107 \quad \dot{E} = \frac{\beta SI}{N} - \sigma E,$$

$$108 \quad \dot{I} = \sigma E - \gamma I,$$

$$109 \quad \dot{H} = \theta \gamma I - \kappa H,$$

$$110 \quad \dot{D} = \delta \kappa H,$$

$$111 \quad \dot{R} = (1 - \theta) \gamma I + (1 - \delta) \kappa H.$$

112 Here,  $S$ ,  $E$ ,  $I$ ,  $R$ ,  $H$ , and  $D$  represent susceptible, exposed, infection, recovered, hospitalized, and death  
113 classes. The parameters  $\beta$ ,  $\sigma$ ,  $\gamma$ ,  $\kappa$  are transmission rate, progression rate from  $E$  to  $I$ , recovery rate (for  
114 fitting simplicity, we assumed the recovery rate and hospitalization rate to be the same), the proportion  
115 of individuals moving from  $H$  to  $D$ , respectively.  $\theta$  represents proportion of hospitalization (or recorded  
116 cases or severe cases) among infection and  $\delta$  represents the proportion of death among hospitalization  
117 (or recorded cases or severe cases). Here, we assumed that hospitalization can be interpreted as  
118 symptomatic cases. Since we do not explicitly incorporate the hospitalization cases in fitting, the exact  
119 definition is not crucial. The infection fatality rate equals  $\delta\theta$ . We consider three scenarios on the choice  
120 of  $\delta$ , including  $\delta = \theta$ ,  $\delta = 0.1$ , and  $\delta = 0.05$ . We fit the daily integrated  $D$  to the reported deaths in  
121 each country. We assume a negative nominal measurement noise in reporting with an over-dispersion  
122 parameter  $\tau$ . We assume a time-varying  $\beta$ , which is an exponential cubic spline function with the  
123 number of nodes as 7, which was evenly distributed over the study period from 1 March 2020 to 18 Feb  
124 2021. The time-varying basic reproductive number is given by  $R_0(t) \approx \beta(t)/\gamma$ . The detailed model-  
125 fitting method can be found in many previous studies (He et al., 2020a; Musa et al., 2020b; Zhao et al.,  
126 2018).

127 In the classic susceptible-exposed-recovered-based models, the mean GI of an infectious disease  
128 equals the sum of the mean latent period (LP) and the mean infectious period (IP) (Svensson, 2007). The  
129 duration of individuals in an exposed/infectious class follows exponential distributions. Due to the  
130 discrete-time in the simulation of the model, the realized (or simulated) mean LP and mean IP according  
131 to He et al. (He et al., 2010), are  $LP = \frac{\delta}{1-e^{-\delta\sigma}}$ ,  $IP = \frac{\delta}{1-e^{-\delta\gamma}}$ , where  $\delta$  designate the time discretization  
132 step. Thus  $\sigma^{-1}$  and  $\gamma^{-1}$  are theoretical mean LP and IP. The simulated periods were slightly larger than  
133 theoretical values due to the time discretization. The discrepancy diminishes when the time step size  
134 approaches zero. Hence, the sum of the mean LP and mean IP is estimated at 6.07 days with a 1-day  
135 time step size and theoretical 2 days LP and 3 days IP. The mean GI equals 5 days when the time step  
136 size approaches zero. Besides  $\sigma^{-1}$  at 2 days and  $\gamma^{-1}$  at 3 days, we set  $\kappa^{-1}=14$  days and  $\theta^2$  in the range  
137 of 0.5% to 1% (Mellan et al., 2020). All these parameter values are biologically reasonable.

138 Therefore, using iterated filtering methods, we fitted a SEIRD model with an additional death  
139 class to reported COVID-19 deaths in the three countries (i.e., Belgium, Israel, and UAE) to reveal the  
140 effects of the mean LP and the mean IP on the estimation of reproduction number. We fitted the model

141 to COVID-19 deaths data since COVID-19 mortality data seems less affected by testing policy  
142 compared to other diseases.

## 143 **Results and discussion**

144 Based on a recent study on GI and SI, we observed that most studies showed that the SI (and/or  
145 GI) of COVID-19 varies between 5-6 days (Griffin et al., 2020). In particular, Ferretti et al. (Ferretti et  
146 al., 2020) reported the mean GI as 5.0 days, Ganyani et al. (Ganyani et al., 2020b) used the data for  
147 Singapore and Tianjin, China, and found that the mean GI is estimated at 5.20 (3.78 – 6.78) days and  
148 3.95 (3.01 – 4.91) days, respectively. In forty research papers reviewed by Griffin et al. (Griffin et al.,  
149 2020) on the GI and SI, only three studies provided an estimate for the mean GI, which varies roughly  
150 between 3.95 to 5.20 days. And one paper provided an estimate for the median of the GI as 5.0 days  
151 (Backer et al., 2020; Ferguson et al., 2020; Griffin et al., 2020; Li et al., 2020). Furthermore, Zhang et al.  
152 (Zhang et al., 2020) reported that the incubation period of COVID-19 was estimated at 5.2 (95%CI: 1.8-  
153 12.4), and the mean IP at 4.4 (95%CI: 0.0-14.0) from Dec 24 to Jan 27, 2020, and 2.6 (95%CI: 0.0-9.0)  
154 from Jan 28 to Feb 17, 2020.

155 However, several studies reported the period of disease progression before the infectiousness  
156 stage as the LP in an SEIR epidemic model. For example, Yin et al. (Yin et al., 2021) conducted a  
157 modelling study to assess the effectiveness of NPIs measures (including contact tracing, facemask  
158 wearing, and rapid testing) to curtail the spread of the COVID-19 in China. They reported that  
159 asymptomatic patients lasted 4.6 days in LP and 9.5 days in IP until removal. See **Table 1** for more  
160 details. Many studies did not follow the rule that  $\text{mean GI} = \text{mean LP} + \text{mean IP} < 6$  days. Therefore, we  
161 emphasized that appropriate use of the generation interval in an epidemiological study is essential to  
162 effectively control the COVID-19 outbreaks, because it provides a more accurate estimate on  
163 reproduction number for the epidemics, and is crucial for pandemic mitigation planning and forecasting.

164 For demonstration purposes, we compared epidemiologic dynamics of COVID-19 for some  
165 randomly selected countries (Belgium, Israel, and UAE) while varying LP and IP from (2 & 3 days to 3  
166 & 6 days). We employed the model to the COVID-19 mortality data and obtained the time series fitting  
167 results using the COVID-19 data for Belgium, Israel, and UAE to quantify the effects of longer GI on  
168 the estimation of (time-varying) reproduction numbers. In **Figure 2** we show the fitting results of the  
169 daily confirmed COVID-19 deaths (red circled) with proper LP and IP at 2 & 3 days. in (a) Belgium, (b)  
170 Israel, and (c) UAE, respectively. The median of the simulation is represented by the black curve, and

171 the time-varying basic reproduction number is denoted by the blue dashed curve. The 95% range of the  
172 simulation is shown by the shaded gray region. In **Figure 3**, we compare six scenarios, corresponding  
173  $\delta = \theta$ ,  $\delta = 0.1$ , and  $\delta = 0.05$ , with proper GI (LP and IP at 2 & 3 days) versus long GI (LP=3 days and  
174 IP=6 days) for each country. From **Figure 3**, we discovered that using longer mean LP and mean IP  
175 would significantly increase an estimate of reproduction number. Thus, the magnitude of reduction in  
176 the initial reproduction number would be much higher in the latter cases (3&6 days for LP&IP) than in  
177 the proper former cases (2&3 days for LP&IP). Besides, a higher initial reproduction number would  
178 imply a much higher expected infection attack rate and herd immunity threshold.

179 Furthermore, a summary results of the COVID-19 infection attack rates (AR) for Belgium,  
180 Israel, and UAE is presented in **Table 2** with reasonable LP and IP values. The choice of LP and IP had  
181 an important influence on the estimate of AR, likely due to the choice of the flexible transmission rate in  
182 our model, and the assumption of the infection fatality rate which varies between 0.5% to 1%.

183 **Appendix Table 1** presents the results of the estimated parameter values using the log-likelihood  
184 estimation approach for Belgium, Israel, and UAE. We observed that Belgium has the lowest log  
185 likelihood values, indicating that Belgium was hit harder than the other two countries. also, a summary  
186 results of the estimated values for the time-varying transmission rate with a fixed number of nodes  
187 (denoted by  $n_m$ ) was given in **Appendix Table 2**. The initial values for the state variables used for the  
188 model given in **Appendix Table 3**. Therefore, based on the results obtained and the comparison of the  
189 epidemic dynamics of COV-ID-19 for Belgium, Israel, and UAE with varying LP and IP, we argue that  
190 appropriate LP and IP should be used in epidemiological modelling study to effectively mitigate the  
191 spread of disease and to provide suitable suggestions of control strategies for public health  
192 implementation and policymaking.

## 193 **Conclusions**

194 Mean LP, IP, and GI are essential quantities in epidemiological modelling studies that are used  
195 for the estimation of reproductive number of an infectious disease. For COVID-19, current knowledge  
196 showed that the mean GI (mean LP + mean IP) varies between 5-6 days, which implies that the mean  
197 LP/IP in SEIR models should be around 2-3 days, respectively. We emphasized that this estimate should  
198 be used to provide a reasonable estimation of the reproductive number ( $R_0$ ), which helps in  
199 policymaking to curtail the spread of an infectious disease. We showed that the estimated  $R_0(t)$  for  
200 Belgium, Israel, and UAE are elevated substantially when longer LP and IP are used. Since now

201 vaccination programs are ongoing in these countries, all modeling fitting is timely to lay the groundwork  
202 for the efficacy evaluation of the vaccination programs in these countries.

203

204

205

206

207 **Declarations**

208 **Ethical approval and consent to participate**

209 Not applicable.

210 **Consent for publication**

211 Not applicable.

212 **Availability of data and materials**

213 All data used are publicly available.

214 **Conflict of interests**

215 DH was supported by an Alibaba (China) Co. Ltd Collaborative Research Project. Other authors  
216 declared no conflict of interests.

217 **Funding**

218 DH was supported by an Alibaba (China) Co. Ltd Collaborative Research grant (ZG9Z). The funder had  
219 no role in study design, data collection and analysis, decision to publish, or preparation of the  
220 manuscript.

221

222 **Author contributions**

223 All authors contributed equally for this manuscript.

224 **Acknowledgements**

225 Not applicable.

226

227

## 228 **References**

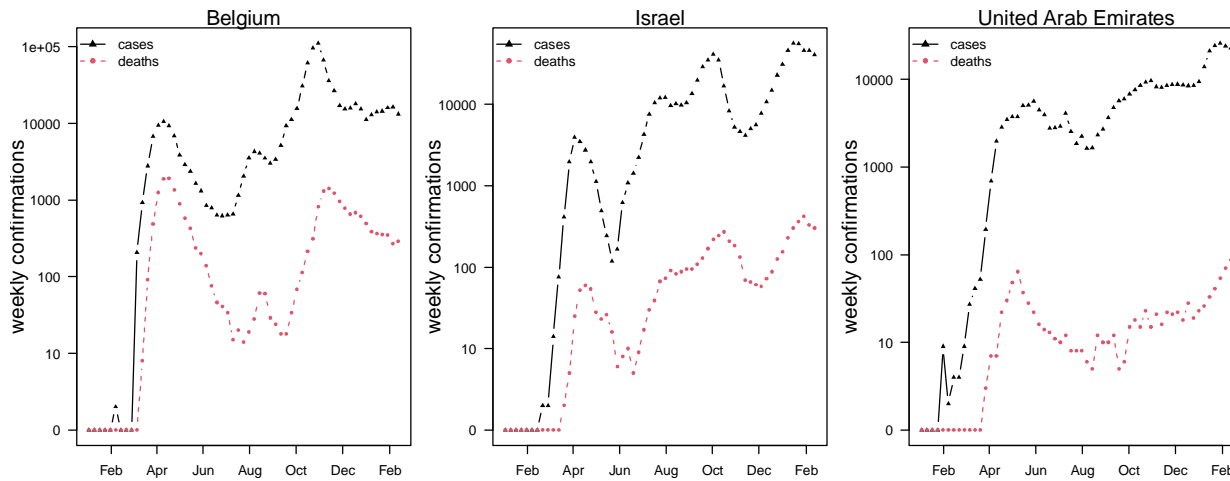
### 229 **Uncategorized References**

- 230 Ali, S. T., Wang, L., Lau, E. H., Xu, X.-K., Du, Z., Wu, Y., Leung, G. M., Cowling, B. J., 2020. Serial  
231 interval of SARS-CoV-2 was shortened over time by nonpharmaceutical interventions. *Science*  
232 369, 1106-1109.
- 233 Backer, J. A., Klinkenberg, D., Wallinga, J., 2020. Incubation period of 2019 novel coronavirus (2019-  
234 nCoV) infections among travellers from Wuhan, China, 20–28 January 2020. *Eurosurveillance*  
235 25, 2000062.
- 236 Du, Z., Xu, X., Wu, Y., Wang, L., Cowling, B. J., Meyers, L. A., 2020. Serial Interval of COVID-19  
237 among Publicly Reported Confirmed Cases. *Emerg Infect Dis* 26, 1341-1343,  
238 doi:10.3201/eid2606.200357.
- 239 Emery, J. C., Russel, T. W., Liu, Y., Hellewell, J., Pearson, C. A., Knight, G. M., Eggo, R. M.,  
240 Kucharski, A. J., Funk, S., Flasche, S., 2020. The contribution of asymptomatic SARS-CoV-2  
241 infections to transmission—a model-based analysis of the Diamond Princess outbreak. *medRxiv*.
- 242 Ferguson, N., Laydon, D., Nedjati Gilani, G., Imai, N., Ainslie, K., Baguelin, M., Bhatia, S., Boonyasiri,  
243 A., Cucunuba Perez, Z., Cuomo-Dannenburg, G., 2020. Report 9: Impact of non-pharmaceutical  
244 interventions (NPIs) to reduce COVID19 mortality and healthcare demand. Imperial College  
245 London, 1-20, doi:10.25561/77482.
- 246 Ferretti, L., Wymant, C., Kendall, M., Zhao, L., Nurtay, A., Abeler-Dörner, L., Parker, M., Bonsall, D.,  
247 Fraser, C., 2020. Quantifying SARS-CoV-2 transmission suggests epidemic control with digital  
248 contact tracing. *Science* 368.
- 249 Ganyani, T., Kremer, C., Chen, D., Torneri, A., Faes, C., Wallinga, J., Hens, N., 2020a. Estimating the  
250 generation interval for coronavirus disease (COVID-19) based on symptom onset data, March  
251 2020. *Euro Surveill* 25, 2000257, doi:10.2807/1560-7917.ES.2020.25.17.2000257.
- 252 Ganyani, T., Kremer, C., Chen, D., Torneri, A., Faes, C., Wallinga, J., Hens, N., 2020b. Estimating the  
253 generation interval for coronavirus disease (COVID-19) based on symptom onset data, March  
254 2020. *Eurosurveillance* 25, 2000257.
- 255 Griffin, J., Casey, M., Collins, Á., Hunt, K., McEvoy, D., Byrne, A., McAloon, C., Barber, A., Lane, E.  
256 A., More, S., 2020. Rapid review of available evidence on the serial interval and generation time  
257 of COVID-19. *BMJ open* 10, e040263.
- 258 He, D., Ionides, E. L., King, A. A., 2010. Plug-and-play inference for disease dynamics: measles in large  
259 and small populations as a case study. *Journal of the Royal Society Interface* 7, 271-283.
- 260 He, D., Zhao, S., Lin, Q., Musa, S. S., Stone, L., 2020a. New estimates of the Zika virus epidemic attack  
261 rate in Northeastern Brazil from 2015 to 2016: A modelling analysis based on Guillain-Barré  
262 Syndrome (GBS) surveillance data. *PLoS neglected tropical diseases* 14, e0007502.
- 263 He, X., Lau, E. H., Wu, P., Deng, X., Wang, J., Hao, X., Lau, Y. C., Wong, J. Y., Guan, Y., Tan, X.,  
264 2020b. Temporal dynamics in viral shedding and transmissibility of COVID-19. *Nature*  
265 *medicine* 26, 672-675.
- 266 Kissler, S. M., Tedijanto, C., Goldstein, E., Grad, Y. H., Lipsitch, M., 2020. Projecting the transmission  
267 dynamics of SARS-CoV-2 through the postpandemic period. *Science* 368, 860-868.
- 268 Kong, D., Zheng, Y., Wu, H., Pan, H., Wagner, A. L., Zheng, Y., Gong, X., Zhu, Y., Jin, B., Xiao, W.,  
269 Mao, S., Lin, S., Han, R., Yu, X., Cui, P., Jiang, C., Fang, Q., Lu, Y., Fu, C., 2020. Pre-  
270 symptomatic transmission of novel coronavirus in community settings. *Influenza Other Respir*  
271 *Viruses* 14, 610-614, doi:10.1111/irv.12773.

- 272 Lauer, S. A., Grantz, K. H., Bi, Q., Jones, F. K., Zheng, Q., Meredith, H. R., Azman, A. S., Reich, N. G.,  
273 Lessler, J., 2020. The incubation period of coronavirus disease 2019 (COVID-19) from publicly  
274 reported confirmed cases: estimation and application. *Annals of internal medicine* 172, 577-582.
- 275 Li, Q., Guan, X., Wu, P., Wang, X., Zhou, L., Tong, Y., Ren, R., Leung, K. S., Lau, E. H., Wong, J. Y.,  
276 2020. Early transmission dynamics in Wuhan, China, of novel coronavirus–infected pneumonia.  
277 *New England journal of medicine*.
- 278 Lipsitch, M., Cohen, T., Cooper, B., Robins, J. M., Ma, S., James, L., Gopalakrishna, G., Chew, S. K.,  
279 Tan, C. C., Samore, M. H., 2003. Transmission dynamics and control of severe acute respiratory  
280 syndrome. *science* 300, 1966-1970.
- 281 Mellan, T. A., Hoeltgebaum, H. H., Mishra, S., Whittaker, C., Schnekenberg, R. P., Gandy, A., Unwin,  
282 H. J. T., Vollmer, M. A., Coupland, H., Hawryluk, I., 2020. Subnational analysis of the COVID-  
283 19 epidemic in Brazil. *MedRxiv*.
- 284 Musa, S. S., Zhao, S., Wang, M. H., Habib, A. G., Mustapha, U. T., He, D., 2020a. Estimation of  
285 exponential growth rate and basic reproduction number of the coronavirus disease 2019  
286 (COVID-19) in Africa. *Infectious diseases of poverty* 9, 1-6.
- 287 Musa, S. S., Zhao, S., Gao, D., Lin, Q., Chowell, G., He, D., 2020b. Mechanistic modelling of the large-  
288 scale Lassa fever epidemics in Nigeria from 2016 to 2019. *Journal of theoretical biology* 493,  
289 110209.
- 290 Nishiura, H., Linton, N. M., Akhmetzhanov, A. R., 2020. Serial interval of novel coronavirus (COVID-  
291 19) infections. *International journal of infectious diseases* 93, 284-286.
- 292 Park, S. W., Sun, K., Viboud, C., Grenfell, B. T., Dushoff, J., 2020. Potential role of social distancing in  
293 mitigating spread of coronavirus disease, South Korea. *Emerging infectious diseases* 26, 2697.
- 294 Ren, X., Li, Y., Yang, X., Li, Z., Cui, J., Zhu, A., Zhao, H., Yu, J., Nie, T., Ren, M., Dong, S., Cheng,  
295 Y., Chen, Q., Chang, Z., Sun, J., Wang, L., Feng, L., Gao, G. F., Feng, Z., Li, Z., 2020. Evidence  
296 for pre-symptomatic transmission of coronavirus disease 2019 (COVID-19) in China. *Influenza  
297 Other Respir Viruses* 15, 19-26, doi:10.1111/irv.12787.
- 298 Svensson, Å., 2007. A note on generation times in epidemic models. *Mathematical biosciences* 208,  
299 300-311.
- 300 Tindale, L. C., Stockdale, J. E., Coombe, M., Garlock, E. S., Lau, W. Y. V., Saraswat, M., Zhang, L.,  
301 Chen, D., Wallinga, J., Colijn, C., 2020. Evidence for transmission of COVID-19 prior to  
302 symptom onset. *Elife* 9, e57149, doi:10.7554/eLife.57149.
- 303 Wallinga, J., Lipsitch, M., 2007. How generation intervals shape the relationship between growth rates  
304 and reproductive numbers. *Proceedings of the Royal Society B: Biological Sciences* 274, 599-  
305 604, doi:10.1098/rspb.2006.3754.
- 306 Wang, X., Pasco, R. F., Du, Z., Petty, M., Fox, S. J., Galvani, A. P., Pignone, M., Johnston, S. C.,  
307 Meyers, L. A., 2020. Impact of social distancing measures on coronavirus disease healthcare  
308 demand, central Texas, USA. *Emerging infectious diseases* 26, 2361.
- 309 WHO, 2021. World Health Organization. Coronavirus disease ( COVID-19).
- 310 WM, 2021. Worldmeter. Population.
- 311 Yan, P., 2008. Separate roles of the latent and infectious periods in shaping the relation between the  
312 basic reproduction number and the intrinsic growth rate of infectious disease outbreaks. *Journal  
313 of theoretical biology* 251, 238-252.
- 314 Yin, L., Zhang, H., Li, Y., Liu, K., Chen, T., Luo, W., Lai, S., Li, Y., Tang, X., Ning, L., 2021.  
315 Effectiveness of Contact Tracing, Mask Wearing and Prompt Testing on Suppressing COVID-19  
316 Resurgences in Megacities: An Individual-Based Modelling Study.

- 317 Zhang, J., Litvinova, M., Wang, W., Wang, Y., Deng, X., Chen, X., Li, M., Zheng, W., Yi, L., Chen, X.,  
318 2020. Evolving epidemiology and transmission dynamics of coronavirus disease 2019 outside  
319 Hubei province, China: a descriptive and modelling study. *The Lancet Infectious Diseases* 20,  
320 793-802.
- 321 Zhao, S., 2020. Estimating the time interval between transmission generations when negative values  
322 occur in the serial interval data: using COVID-19 as an example. *Mathematical biosciences and*  
323 *engineering* 17, 3512-3519.
- 324 Zhao, S., Stone, L., Gao, D., He, D., 2018. Modelling the large-scale yellow fever outbreak in Luanda,  
325 Angola, and the impact of vaccination. *PLoS neglected tropical diseases* 12, e0006158.
- 326 Zhao, S., Cao, P., Gao, D., Zhuang, Z., Cai, Y., Ran, J., Chong, M. K., Wang, K., Lou, Y., Wang, W.,  
327 2020a. Serial interval in determining the estimation of reproduction number of the novel  
328 coronavirus disease (COVID-19) during the early outbreak. *Journal of travel medicine* 27,  
329 taaa033.
- 330 Zhao, S., Gao, D., Zhuang, Z., Chong, M. K., Cai, Y., Ran, J., Cao, P., Wang, K., Lou, Y., Wang, W.,  
331 2020b. Estimating the serial interval of the novel coronavirus disease (COVID-19): A statistical  
332 analysis using the public data in Hong Kong from January 16 to February 15, 2020. *Frontiers in*  
333 *Physics* 8.  
334  
335  
336

337 **Figures**

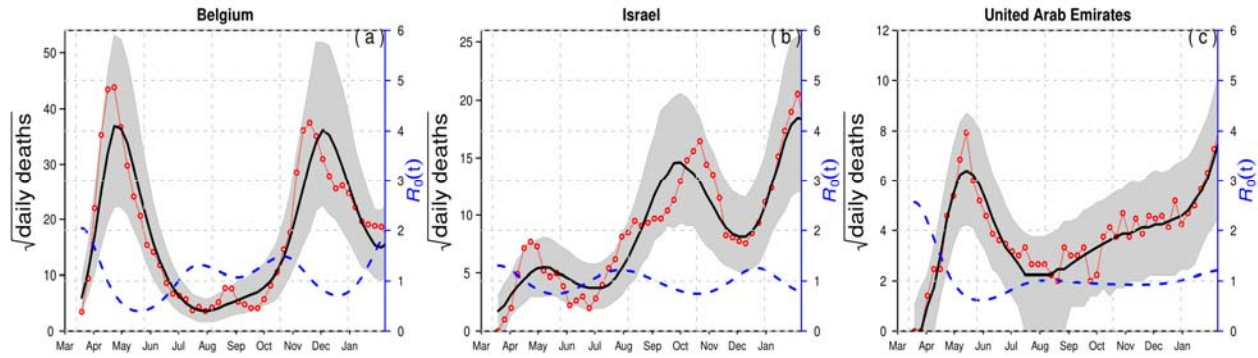


338

339 **Figure 1:** Weekly confirmed cases (in black triangles) and deaths (in red triangles) of COVID-19 in  
340 Belgium, Israel, and the United Arab Emirates.

341

342

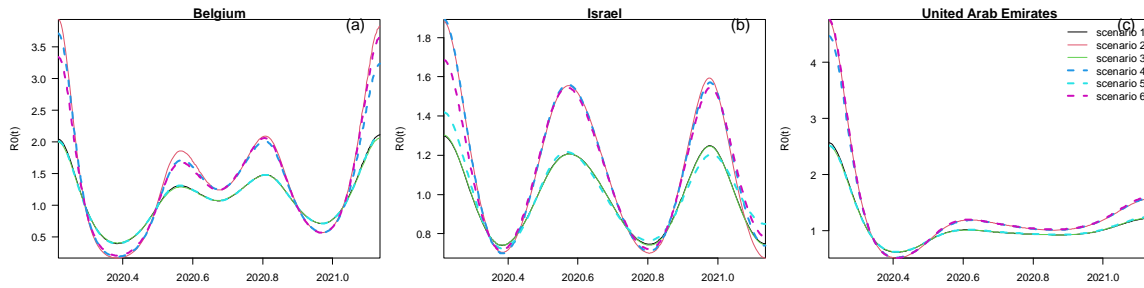


343

344 **Figure 2:** Time series fitting results of daily confirmed COVID-19 deaths (in red circled) in (a)  
345 Belgium, (b) Israel and (c) the United Arab Emirates represented, respectively. The medium of the  
346 simulation is represented by the black curve, and the time varying reproduction number ( $R_0(t)$ ) is  
347 denoted in blue dashed curve. The 95% confidence interval of the simulation is shown by the shaded  
348 (gray) region. The mean LP = 2 days and the mean IP = 3 days. Thus, the mean GI = 5 days.

349

350



351

352 **Figure 3:** Comparison of reconstructed  $R_0(t)$  under six different scenarios for three countries (a)  
353 Belgium, (b) Israel and (c) the United Arab Emirates, respectively. The mean LP = 2 days and the mean  
354 IP = 3 days in scenarios 1,2,3. We assumed  $\delta = \theta$  in scenario 1&2, while we fix  $\delta = 0.1$  in scenario  
355 3&4, and  $\delta = 0.05$  in scenario 5&6, respectively. The mean LP = 3 days and the mean IP = 6 days in  
356 scenarios 2,4,6, thus GI=9 days. In all countries, the reconstructed  $R_0(t)$  with longer GI is evidently  
357 higher than that with a shorter GI. If the initial drop of  $R_0(t)$  is associated with control measure, the  
358 assessment with a longer GI will lead to overestimated control effectiveness.

359

360

361 **Tables**

362 **Table 1:** Mean latent period and mean infectious period of COVID-19.

Mean LP (days)/ Mean IP (days)	Equivalent Mean GI (days)	References
None	5.0	(Ferretti et al., 2020)
None	5.20 (3.78-6.78) for Singapore & 3.95 (3.01-4.91) for Tianjin, China	(Ganyani et al., 2020b)
5.2 (95% CI: 1.8-12.4) (incubation period)/ 4.4 (95% CI: 0.0-14.0) from Dec 24 to Jan 27, 2020, and 2.6 (95% CI: 0.0-9.0) from Jan 28 to Feb 17, 2020	>5.2	(Zhang et al., 2020)
4.6/9.5	14.1	(Yin et al., 2021)
4.6/5	9.6	(Kissler et al., 2020)
4.3/(5+2.1+2.9=10)	10	(Emery et al., 2020)
5.1 (incubation period) 12 (95% CI: 2-14)	>12	(Lauer et al., 2020)

363

364

365

366

367 **Table 2:** A summary results of the estimated infection attack rates (AR) in Belgium, Israel, and the UAE  
368 by February 18, 2021.

Country	Population	Death	AR
Belgium	11589623	21041	0.182
Israel	8655535	4634	0.059
UAE	9890402	819	0.009

369

370

371

372

373 **Appendices**

374 **Title:** Using proper mean generation intervals in modelling of COVID-19.

375

376 **File name:** Supplementary material 1 - Appendix.docx

377 **Title of data:** Appendix

378 **Description of data:** Contains the following.

379 Appendix Table 1. Summary table of estimation results of the parameters (using log likelihood).

380

381 Appendix Table 1. Summary table of estimation results of the time varying transmission rate with  
382 number of nodes ( $n_m = 7$ ) fixed.

383

384 Appendix Table 2. Summary table for initial values of state variable of the model.

385

386

387 **Appendix Table 1:** Summary table of estimation results of the parameters (using log likelihood).

Country	loglik	loglik.sd	$\sigma$	$\theta$	$\gamma$	$\kappa$	Pop size
Belgium	-284.8281	0.0229	182.5	0.1	121.6667	26.0714	11589623
Israel	-229.7767	0.034	182.5	0.0954	121.6667	26.0714	8655535
UAE	-139.7897	0.0829	182.5	0.0933	121.6667	26.0714	9890402
Belgium	-285.0237	0.026	121.6667	0.0935	60.8333	26.0714	11589623
Israel	-230.729	0.039	121.6667	0.1	60.8333	26.0714	8655535
UAE	-138.8795	0.0593	121.6667	0.0826	60.8333	26.0714	9890402

388

389

390

391

392

393 **Appendix Table 2:** Summary table of estimation results of the time varying transmission rate with  
394 number of nodes ( $n_m = 7$ ) fixed.

log.beta	log.beta1	log.beta2	log.beta3	log.beta4	log.beta5	log.beta6
5.5159	3.9121	4.9633	4.8712	5.1678	4.4799	5.5484
5.0615	4.5097	4.9234	4.8167	4.5318	5.0215	4.5114
5.7429	4.4287	4.6888	4.7855	4.7286	4.7858	4.9997
5.4773	2.3899	4.5058	4.3241	4.797	3.5729	5.4488
4.7398	3.7754	4.4478	4.2501	3.7927	4.5705	3.7169
5.6623	3.6152	4.0472	4.2476	4.1243	4.2418	4.5581

395

396

397 **Appendix Table 3:** Summary table for initial values of state variable of the model.

S.0	E.0	I.0	T.0	D.0	R.0
11010142	4547	4547	455	45	569887
8222758	392	392	39	4	431950
9395882	11	11	1	0	494496
11010142	7231	7231	723	72	564225
8222758	471	471	47	5	431783
9395882	22	22	2	0	494474

398